Macromolecules

ARTICLE

pubs.acs.org/Macromolecules

A Physical and Mechanical Study of Prestressed Competitive Double Network Thermoplastic Elastomers

Naveen K. Singh and Alan J. Lesser*

Polymer Science and Engineering Department, University of Massachusetts, Amherst, Massachusetts 01003, United States

ABSTRACT: A new approach to prepare and characterize prestressed competitive double network elastomeric systems was investigated. A styrene−butadiene−styrene (SBS) triblock copolymer system containing physical cross-links was used to achieve a double network by additional chemical cross-linking using ultraviolet (UV) light. Properties measured from conventional monotonic tensile tests, stress relaxation, thermomechanical, hysteresis, and swelling analysis were investigated and related to their network structure. These double network elastomers show a transition between competitive and collaborative behavior in their mechanical properties at different strain regimes. These elastomers also show lower permanent set in both low and high strain regimes along with lower hysteresis. These networks exhibit lower modulus along with lower coefficient of thermal expansion, still showing lower swelling ratios, which results from a competition between the networks.

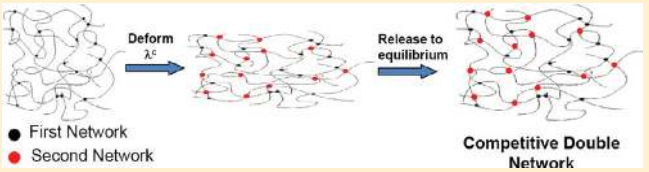

INTRODUCTION

It is well-known that the deformational characteristics of ideal elastomers are mainly governed by entropic response, where energetic contributions are minimal. Whereas for real elastomers, internal energy response can be significant, especially in the low strain regime, due to difference in energy between trans and gauche rotational isomeric states, which can be quite significant, especially in the low strain regime.[1] In the current work, the energetic contributions have been neglected for simplifying the problem.

Consequently, elastomers exchange heat with the surrounding environment upon deformation, which is manifested through a temperature change. A general schematic of this heat exchange during deformation is shown in Figure 1 where heat is emitted from the elastomer to the surroundings while loading and is absorbed while unloading. This heat exchange affects the deformational and thermomechanical properties of these networks, including modulus, maximum elongation, coefficient of thermal expansion, mechanical hysteresis, fatigue life, and permanent set.

One way of utilizing this entropic behavior of these elastomeric networks is to alter the overall heat exchange with the surroundings by completing the curing process on a partially cured elastomer in its deformed state. This second cross-linked network can be formed within the initial network, as depicted in Figure 2. This results in materials with unusual and enhanced properties which have been termed "double-network elastomers" in early literature.[2−6] Recently, Singh and Lesser have reported the formation of these double network elastomers, where the emphasis was given to understanding the thermal and thermomechanical properties of "thermoplastic" elastomers,[7−10] as opposed to traditional chemically cured elastomers which were mainly utilized to understand the aging process and effects of entanglements resulting in permanent set of elastomers under deformation and studying numerous physical and mechanical properties of these elastomers[2,11−22] in various deformation modes including uniaxial extension,[23,24] equibiaxial extension,[25] and shear.[26]

The double network concept, first introduced more than 50 years ago by Tobolsky et al.,[4] was used to explain the physical aging of rubbers, which involved free-radical scission and cross-linking under deformation. The independent network hypothesis that was proposed has shown to be consistent with various experimental results.[24,27−36] This hypothesis suggested that the constitutive relation for postcured networks can be calculated as the sum of the stress contributions from the independent networks, each described by the classical stress−strain expression and each with its own state of equilibrium. The hypothesis covered the whole extension regime and the single model was utilized to predict the overall behavior of the double network elastomers assuming Gaussian behavior.

Flory[27,37] proposed a very general theoretical treatment of similar systems which assumed there are two opposing forces acting on this system. One is due to the network introduced in

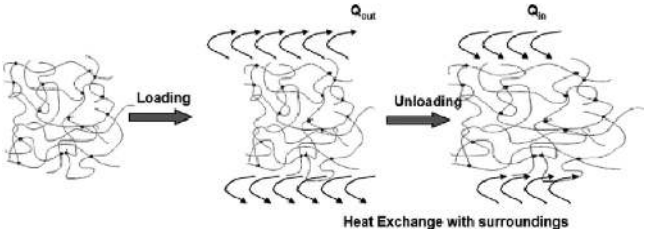

Figure 1. Heat exchange with the surroundings during elastomer deformation.

Received: December 9, 2010
Revised: January 20, 2011
Published: February 15, 2011

Figure 2. Formation of prestressed competitive double network elastomer.

the isotropic state, and the other is due to the network introduced in the strained state; this results in a stress transfer between the networks. This theoretical treatment was later utilized in the Scott−Stein model to explain the deformation behavior of these double network elastomers. James and Guth also proposed a similar model.[38] Various other theoretical treatments were carried out in order to understand the anisotropy and the deformation characteristics of these double network elastomers.[39−47]

The term "double network" used here is different as used in terms of hydrogels as reported recently by Gong et al.,[48,49] where the two networks come from two different monomeric units. The first network is formed from a rigid and brittle polymer, such as polyelectrolyte, whereas the second network is formed by a soft and ductile polymer, such as neutral polymer. The second network being formed while the first network is swollen in the aqueous solution of second polymer. Hence, the double network hydrogels have lower anisotropy while the second network is formed, which depends on swelling ability of first network. Moreover, the nature of two networks is different, whereas the double network elastomers exhibit high anisotropy and the two networks formed can be of the same or different nature depending upon the elastomeric system chosen. These elastomeric networks exhibit a competitive behavior[8] in a low strain regime and hence are termed in this work as "competitive prestressed double network elastomers" in order to make a distinction between the two similar terms used in the literature.

The focus of this work is to understand the physical, mechanical, and thermomechanical behavior of these competitive double network elastomers and their relationship with their network structure. Herein, a competitive double-networked styrene−butadiene−styrene (SBS) triblock copolymer is prepared by utilizing physical cross-links from the hard styrenic phase as the first network and then curing it in a deformed state utilizing the unsaturation of the soft butadiene phase to achieve a second chemically cross-linked network. The tensile, hysteresis, stress relaxation, swelling, and thermomechanical properties of these materials are compared at similar total cross-link times but at different extension ratios before imposing the second network, and the relationships between the different properties along with their dependence on the network structure have been discussed.

EXPERIMENTAL SECTION

Materials. SBS block copolymer (KX405) was obtained from Kraton. The general structure is shown in Figure 3, containing about 24% polystyrene. SBS was mixed with 5% benzophenone (Alfa Aesar), a UV cross-linking initiator, and dissolved in toluene by 5 wt% of polymer. Films with a thickness of ~0.5 mm were obtained after room temperature solvent evaporation and vacuum drying at 50 °C for 6 h. ASTM D1708 tensile samples were punched out of the films.

Competitive Double Network Formation. Double networks of SBS were prepared by UV cross-linking using an Atlas Suntest CPS+. The first network results from the physical cross-links of the hard polystyrene block and is present immediately after processing. The second network was introduced by first uniaxially extending the sample to prescribed extension ratios (λ^c = 1.5, 2, 3, and 4) and subsequently curing it using UV radiation. This one-step UV curing was carried out after optimizing the curing conditions to a dosage power of 700 W/m^2 at 25 °C for 4 h, to give a total dosage of 10 080 kJ/m^2. The optimization determined via UV DSC.[9] After curing, samples were allowed to relax back to their equilibrium state. These double network samples were compared with samples cured at λ^c = 1, which did not undergo any extension between the first and second cure, and also the uncured samples, which contain only the first network of physical cross-links.

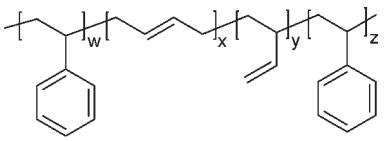

Figure 3. Chemical structure of the polystyrene and polybutadiene blocks (x = cis + trans)[51] of SBS.

Characterization and Testing. *Infrared Spectroscopy.* Fourier transform infrared (FT-IR) spectroscopy was utilized to qualitatively determine the extent of cross-linking in the stretched state. Infrared spectra were obtained with a Perkin-Elmer Spectrum One FTIR spectrometer.

Mechanical Testing. Monotonic uniaxial tensile properties were determined using an Instron 5800 tensile test machine at a constant crosshead speed of 20 mm/min at 23 °C. ASTM D1708 test geometry[8] was employed for all the samples used for mechanical testing. Samples were tested in the direction parallel to the direction of stretch during cure. The engineering stress versus extension ratio curves were plotted for these double networks, where extension ratios (λ^t) were calculated based on the final equilibrium length of these double networks.

Stress relaxation experiments were carried out in low and high strain regimes. The low strain regime experiment was performed on a dynamic mechanical analyzer (TA Instruments, DMA 2980) at a constant extension ratio λ^t = 1.01 at 30 °C for 2 h in tensile mode. The stress relaxation experiment in high strain regime was carried out using an Instron 5800 tensile test machine at a constant λ^t = 1.15 at 30 °C for 2 h in tensile mode.

The hysteresis and Mullins effect in the double network elastomers were studied by a series of cyclic tests. The samples were strained to a prescribed strain and then cycled 20 times at that strain at a rate of 10 mm/min and later stepped to higher strain. The extension ratios λ^t = 1.10, 1.15, and 1.20.

Morphological Characterization. Morphology of the single and double network elastomers after achieving an equilibrium were determined by using small-angle X-ray scattering (SAXS), which was done using an in-house setup from Molecular Metrology Inc. It uses a 30 W microsource (Bede) with a 30 × 30 μm^2 spot size matched to a Maxflux optical system (Osmic) leading to an almost parallel beam of monochromatic Cu Kα radiation (wavelength λ = 0.154 nm). After passing beam-defining and guard pinholes, the beam with a diameter of about 0.5 mm enters the sample chamber. The SAXS intensity is collected by a two-dimensional gas-filled wire detector (mesh size 120 μm) at a distance of 120 cm. A beam-stop of diameter 0.7 mm in front of the detector has in its center a photodiode, allowing monitoring the intensity of the direct beam. The whole system is evacuated. The scattering patterns were recorded at room temperature over a period of 1 h.

Thermomechanical Testing. Thermomechanical properties, including the thermal stability under load and coefficient of thermal expansion, were studied using the film/fiber probe in a TA Instruments thermomechanical analyzer (TMA) 2940CE, at constant load of 0.05 N and heating rate of 3 °C/min.

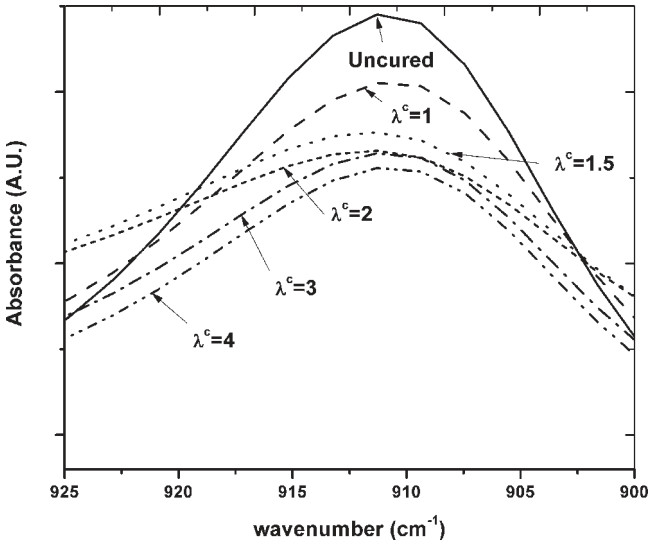

Figure 4. IR spectrum of pendant vinyl group of SBS between 900 and 925 cm^{-1}.

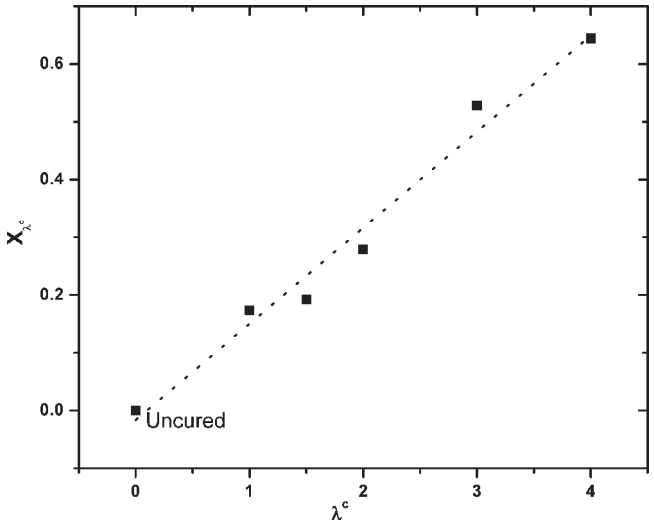

Figure 5. Increase in effective extent of cure during stretch (X_λ^c) with increase in λ^c.

Swelling Characterization. Swelling characteristics of single and double network were determined by swelling the samples in toluene and measuring their weights at different stages of swelling.

RESULTS AND DISCUSSION

Extent of Cross-Linking. The mechanism of free-radical UV cross-linking of SBS has been investigated,[50,51] and it was found that upon exposure to UV the cross-linking takes place via the pendant vinyl groups, while the backbone double bond was unaffected. It was reported that theoretically only three bridges per polymer chain are needed for cross-linking the polymer to infinite molecular weight. Thus, in order to achieve high molecular weight, both intermolecular and intramolecular polymerization processes are expected to take place between vinyl double bonds located on the same polybutadiene chain, leading to the formation of cyclic structures. Moreover, neither cross-linking in the polystyrene phase nor significant vinyl group oxidation is expected, the latter indicated by the carbonyl band at 1694 cm^{-1} in the infrared spectrum. Hence, the photoinitiated polymerization is the main process responsible for the vinyl double bond consumption during the UV irradiation.[50]

The extent of cross-linking was determined qualitatively using infrared spectroscopy. The 910 cm^{-1} peak was chosen as the point of comparison for the different samples because it corresponds to the pendant vinyl unsaturation which undergoes cross-linking as discussed above. The peak corresponding to the backbone unsaturation at 967 cm^{-1} does not show any significant change, which further indicates that the cross-linking takes place via pendant vinyl group rather than the backbone vinyl group. It is observed that, as shown in Figure 4, the 910 cm^{-1} peak intensity decreases with an increase in λ^c, thus indicating a linear increase in the extent of curing which is calculated based on eq 1, to form the second network with the similar curing conditions as shown in Figure 5.

$$X_\lambda{}^c = (A_{\text{uncured}} - A_\lambda{}^c)_{910} \qquad (1)$$

where $X_\lambda{}^c$ is the effective extent of cure in stretched state, A_λ^c the area under the IR peak between 900 and 925 cm^{-1} for sample cured at λ^c, and A_{uncured} the area under the IR peak between 900 and 925 cm^{-1} for the uncured sample.

The increase in effective extent of curing during stretch, as measured by IR absorbance, can be attributed to decrease in thickness and increase in surface area available for UV cross-linking when the samples are stretched to higher λ^c. As UV cross-linking is governed by the diffusion, a lower thickness will lead to a higher extent of cure.

Tensile Response. Figure 6 shows the uniaxial engineering stress versus λ^t curves for the SBS double network systems. Samples tested were single network (uncured) and double networks prepared at λ^c =1, 1.5, 2, 3, and 4. A significant improvement is seen in the mechanical properties of double networks formed in a stretched state as opposed to an unstretched state (λ^c = 1). It is evident from Figure 6a that the double network samples exhibit higher ultimate stress (σ_b) as compared to the λ^c = 1 network which follows the increase in extent of cross-linking with increase in λ^c as shown in Figure 7. This agrees with the independent network hypothesis proposed by Tobolsky. As compared to the uncured sample, σ_b for the double network elastomers is lower, as the uncured sample being tougher can achieve strain hardening, leading to increase in σ_b. Moreover, increase in extent of curing with increase in λ^c results in decrease in maximum strain at break. This can be attributed to limited extensibility of the highly cross-linked network and reduced ability to blunt a crack. Analyzing the data carefully, it is evident from Figure 6b that there is a transition in modulus detectable in the double network elastomer with respect to the single network sample cured at λ^c = 1.

In order to understand the transition point, a plot of stress versus apparent λ is plotted and shown in Figure 8, where $\lambda = \lambda^t \times \lambda^r$, λ^t is the extension ratio during test, λ^r is the residual extension ratio (l_s/l_0), l_s is the set length after curing and releasing, and l_0 is the initial length before stretching for cure. From Figure 8 it is evident that the transition point for each double network sample corresponds to λ^c. This is due to the fact that, for $\lambda < \lambda^c$ for each sample, the two networks are in competition with each other, which results in decrease in modulus even with increase in extent of cross-linking. This decrease in modulus has been observed by Roland et al.[3] For $\lambda > \lambda^c$, they

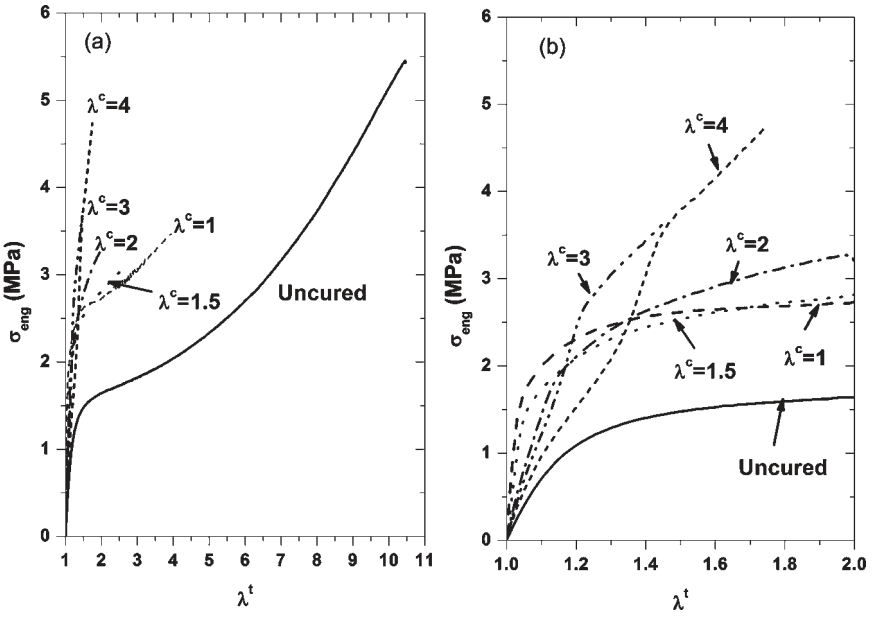

Figure 6. Tensile results of SBS samples cured at different λ^c. (a) Full stress-extension results. (b) Close-up of low-extension regime.

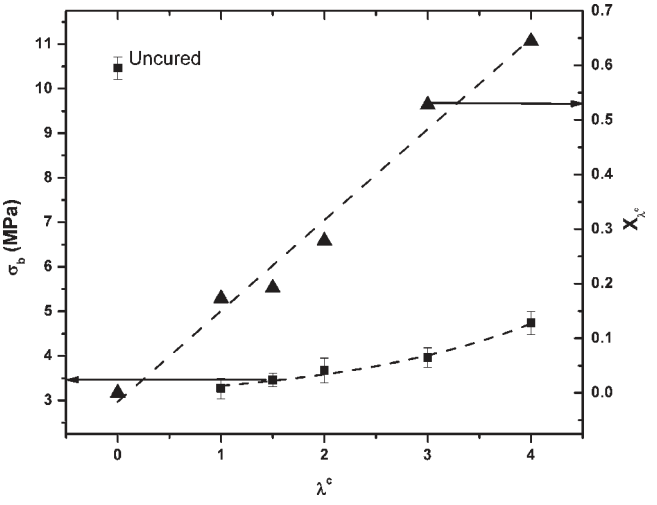

Figure 7. Increase in σ_b with increase in extent of cure during stretch (X_λ^c) with increase in λ^c.

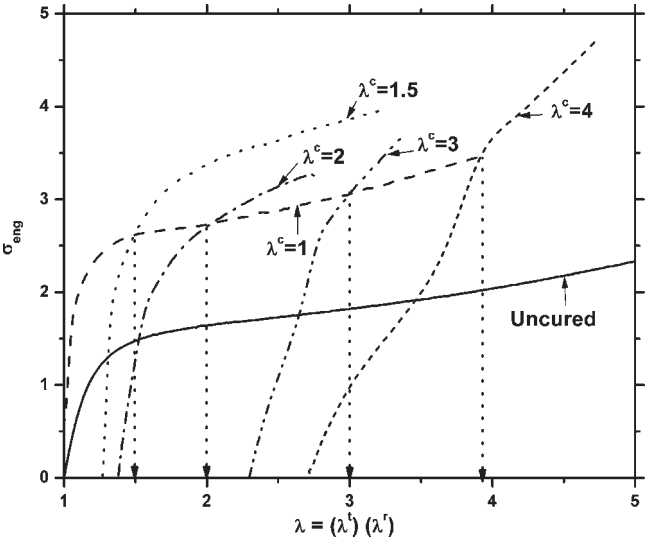

Figure 8. Plot of σ_{eng} vs apparent λ, indicating the transition points in the double network elastomers.

become collaborative and act in parallel where one network is predeformed at an effective strain, leading to an increase in modulus as shown in Figure 9. The increase in modulus beyond the transition point can also be attributed to the stretching of chevron pattern formed in cylindrically separated triblock copolymers[52] and will be discussed later.

Morphology of Prestressed Double Network Elastomers. The phase morphology of the samples was studied using SAXS. The 2-D scans of SAXS are shown in Figure 10. It is observed that with increase in λ^c there is an increase in anisotropy in the cylindrical domains of the SBS triblock copolymer indicated by the elliptical cross-pattern which is permanently set in the double network elastomers. This pattern is attributed to the herring-bone/chevron structure of cylinders[52] at higher strains. This anisotropic set can be attributed to different strain dependencies of the retractive forces of the first network and the network formed in the second stage as observed earlier by Ferry et al.[29]

The rotation of polystyrene cylinders at higher strain leads to the cross-pattern as shown in Figure 11. This rotation leads to shear of the elastomeric phase constrained between the cylinders[52] contributing to increase in modulus beyond the transition point along with the collaborative behavior of the two networks formed within the elastomeric phase.

Stress Relaxation. Stress relaxation of uncured and single network styrenic based triblock systems has been studied earlier.[53−56] However, this investigation deals with relaxation behavior of the competitive double network elastomers based on SBS triblock copolymer. The three main aspects studied are (i) stress relaxation at constant deformation below and above the competitive−collaborative transition point as mentioned before (i.e., in the high and low strain regimes, respectively) and subsequent strain recovery, (ii) stress relaxation rates and overall times for the relaxation process, and (iii) permanent set

dx.doi.org/10.1021/ma1028054 |*Macromolecules* 2011, 44, 1480–1490

represented by that part of the original deformation which is never recovered.

Stress Relaxation in Low Strain Regime. The uncured sample, the sample cured at $\lambda^c = 1$, and the competitive double network samples cured at $\lambda^c = 1.5-4$ were strained to $\lambda^t = 1.01$ extension ratio in DMA and were allowed to relax for 2 h. The stress−relaxation data were analyzed using the procedure X reported by Tobolsky et al.[57] which was adapted for styrene-based triblock copolymers by Wu et al.[54] and Winter et al.[58] The stress relaxation of SBS copolymer is related to number of network chains for a chemically cross-linked system by a discrete distribution:

$$\frac{\sigma(t)}{\sigma(0)} = \sum_{i=1}^{n}\left[\frac{\sigma_i(0)}{\sigma(0)}\exp\left(-\frac{t}{\tau_i}\right)\right] \quad (2)$$

where t is time and $\sigma(t)$ and $\sigma(0)$ are the stresses at $t = t$ and $t = 0$. respectively. τ_n are time constants for relaxation processes. A plot of $\ln(\sigma(t)/\sigma(0))$ vs t should approach a straight line for $t > \tau_n$ if a maximum relaxation time truly exists. The intercept of the line is $\ln(\sigma_n(0)/\sigma(0))$; the slope of the line is $-1/\tau_n$. Equation 2 can be written in the form

$$\frac{\sigma(t)}{\sigma(0)} - \frac{\sigma_n(0)}{\sigma(0)}\exp\left(-\frac{t}{\tau_n}\right) = \sum_{i=1}^{n-1}\left[\frac{\sigma_i(0)}{\sigma(0)}\exp\left(-\frac{t}{\tau_i}\right)\right] \quad (3)$$

A plot of

$$\ln\left(\frac{\sigma(t)}{\sigma(0)} - \frac{\sigma_n(0)}{\sigma(0)}\exp\left(-\frac{t}{\tau_n}\right)\right)$$

versus t should also lead to a straight line for $t > \tau_{n-1}$ if there exists a true discrete relaxation time for $\tau_{n-1} < t < \tau_n$. The process can be repeated for $i = n - 2$, etc., following the determination of the slope and the intercept, discussed above for SBS triblock system $n = 3$. Hence, the time constants τ_1, τ_2, and τ_3, correspond to three processes causing stress relaxation. They are (i) physical flow from the elastomeric phase, (ii) physically trapped confinements, and (iii) the conformational change of the phenyl ring side group in the polystyrene cylindrical domain.[59] It has been reported that $\tau_1 < \tau_2 < \tau_3$, which suggests that physical flow is the fastest relaxation process while the relaxation of domains is the slowest. The procedure is found to be a good fit for the data as shown in Figure 12.

The three time constants (τ_1, τ_2, and τ_3) are plotted with respect to λ^c as shown in Figure 13. It is observed that, in the low strain regime, the time constants τ_1 and τ_3, corresponding to physical flow and the conformational change of the phenyl ring side group in the polystyrene cylindrical domain, both increase with an increase in λ^c. This increase can be attributed to an

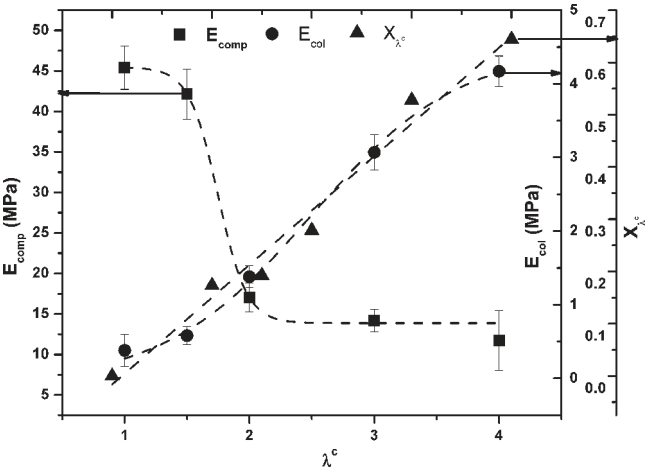

Figure 9. Modulus in low strain (E_{comp}) and high strain (E_{col}) regimes along with increase in extent of cure during stretch (X_λ^c) with increasing λ^c.

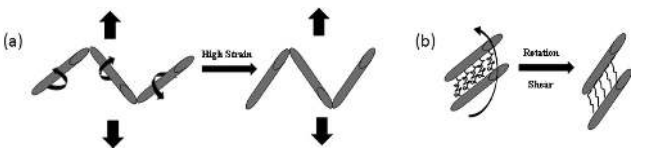

Figure 11. Schematic representation showing (a) rotation of bent PS-cylinders and (b) imposed shear deformation in rubbery phase due to the rotation of PS-domains.[52]

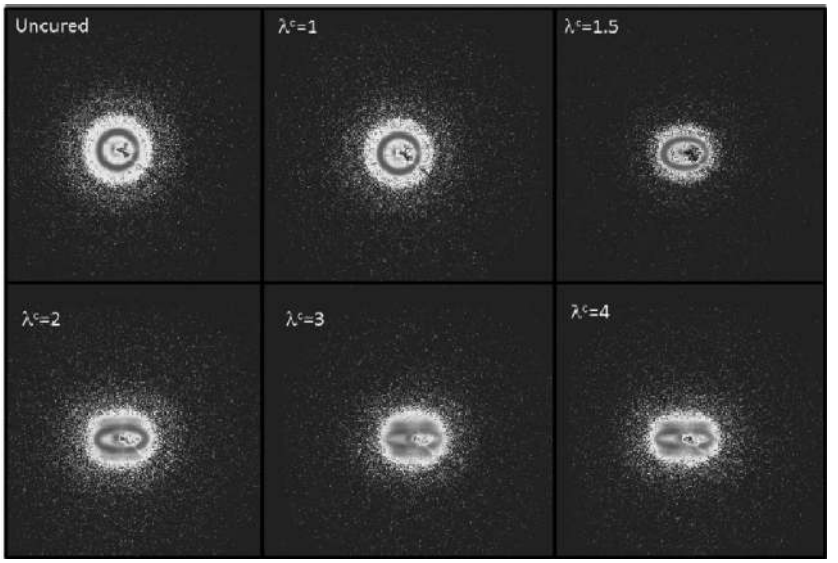

Figure 10. SAXS images of the single and double network elastomers.

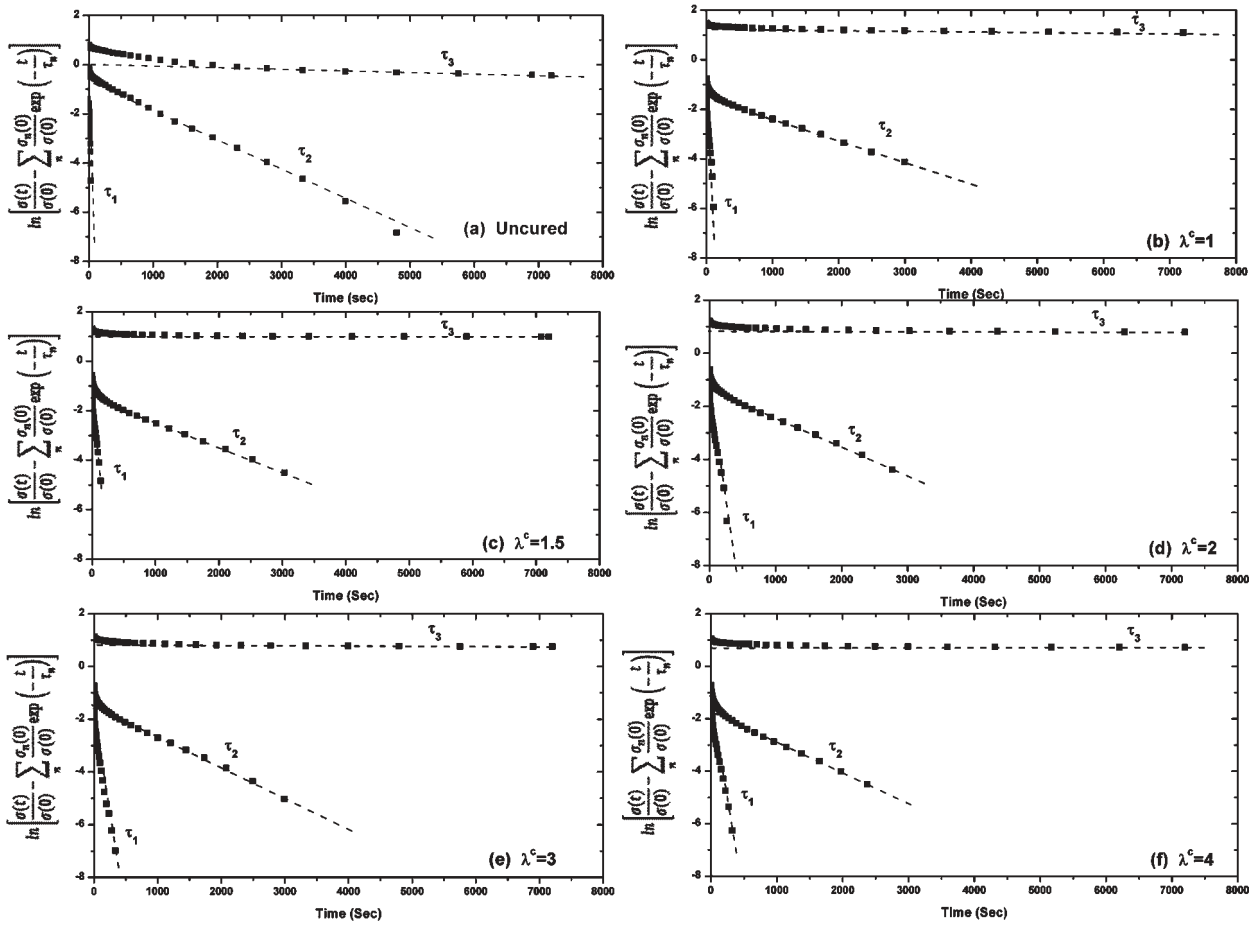

Figure 12. Separation of stress relaxation of double and single network elastomers using procedure X in low strain regime.

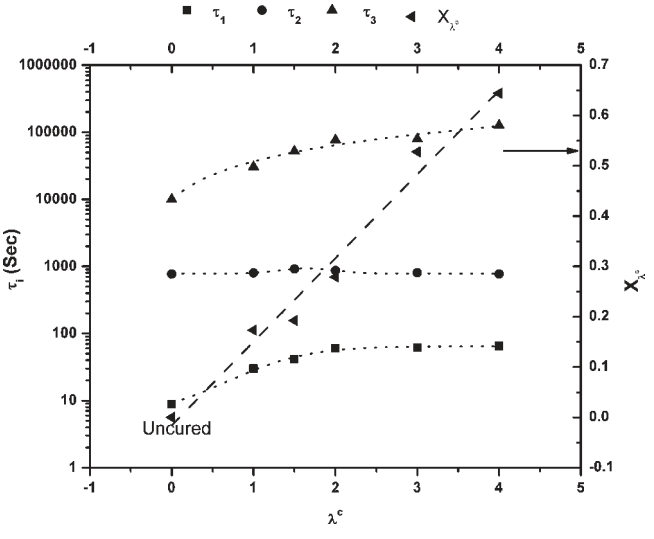

Figure 13. Time constants τ_1, τ_2, and τ_3 as a function of λ^c and their relationship with extent of cure during stretch (X_λ^c) in low strain regime.

increase in degree of cross-linking with increase in λ^c, leading to increase in constraints on the chains of both polystyrene and polybutadiene phases. The polystyrene phase is effected as the orientation relaxation takes place due to formation of the chevron patterns, and the stability and number of the patterns will depend on the ability of the system to hold the chevron patterns (or have higher permanent set). Hence, an increase in cross-linking of butadiene phase (leading to an increase in permanent set) will lead to increase in ability of the system to sustain more oriented chevron patterns, which can relax at longer times by phenyl group flips.[59] Hence, the number of phenyl groups which can undergo the phenyl flips increases. In contrast, the time constant τ_2 is essentially constant because the relaxation of trapped confinements from first network is balanced by the relaxation of trapped confinements in the second network within the competitive regime. Further, these confinements are not sheared to high extent between polystyrene domains at low λ^t and show a similar relaxation behavior for samples at all the values of λ^c.

Strain Recovery in Low Strain Regime. Permanent set in the samples was measured by performing a strain recovery experiment in the DMA for 30 min after stress relaxation experiment described in the previous section. Figure 14 shows the strain recovery with respect to time. It is observed that with an increase in λ^c there is an increase in the recovery rate, as shown in Figure 15. This increase in recovery rate can be attributed to the fact that relaxation process is dominated by physical relaxations, and with increase in λ^c, there is an increase in rate of achieving equilibrium due to increase in competitive nature of the two networks. This faster recovery results in a decrease in permanent set of these competitive double network elastomers with increase in λ^c in low strain regime.

Stress Relaxation in High Strain Regime. The uncured sample, the sample cured at $\lambda^c = 1$, and the competitive network

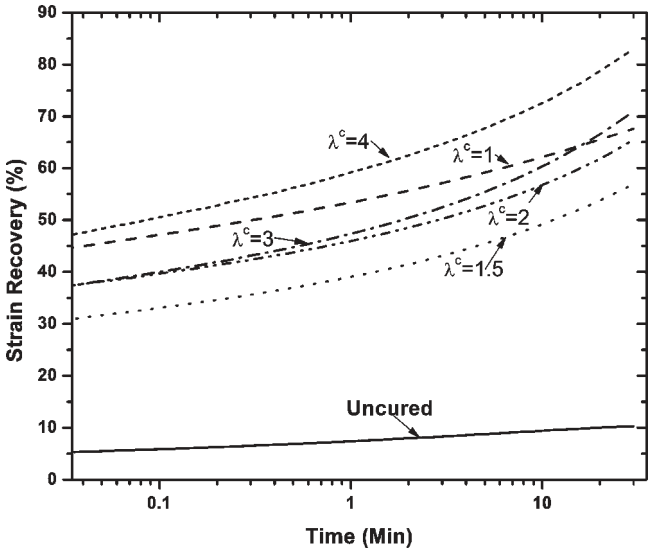

Figure 14. Strain recovery after stress relaxation experiment.

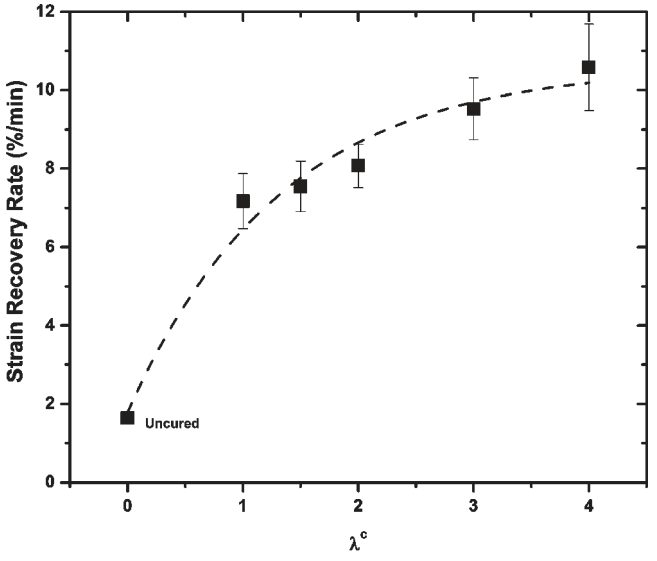

Figure 15. Increase in strain recovery rate with increase in λ^c.

samples cured at $\lambda^c = 1.5-4$ were strained to $\lambda^t = 1.15$ extension ratio at 50 mm/min and were allowed to relax for 2 h. The stress−relaxation data were discretely fitted again using the procedure X given in eq 3. The procedure is found to be a good fit for the data and is shown in Figure 16.

The three time constants (τ_1, τ_2, and τ_3) are plotted with respect to λ^c as shown in Figure 17. It is observed that even in the high strain regime the time constants τ_1 and τ_3, corresponding to physical flow and the conformational change of the phenyl ring side group in the polystyrene cylindrical domain, increase with increase in λ^c, and this increase can be attributed to the increase in degree of cross-linking with increase in λ^c. Whereas, the time constant τ_2 shows different behavior as compared to low strain regime. The time constant τ_2 is almost constant between uncured and cured at $\lambda^c = 1$. Hence, it is clear that this time constant is independent of degree of cross-linking but is dependent on the strain during cross-linking (λ^c) in high strain regime. It is evident from Figure 17 that with an increase in λ^c there is a decrease in τ_2. This can be attributed to the fact that beyond the transition point physically trapped confinements from both networks can relax together, and as the apparent strain increases with λ^c, the rate of relaxation increases. Furthermore, at higher strain the apparent shear on the trapped confinements between the polystyrene cylinders increases with λ^c and hence contributing to an increase in rate of relaxation.

Instantaneous Recovery in High Strain Regime. Instead of carrying out strain recovery experiment in the high strain regime, instantaneous set and permanent set were calculated by measuring various lengths, before and after the stress relaxation experiment.

The instantaneous set can be calculated by means of the two-network hypothesis of Tobolsky et al.[4] The relation for instantaneous set (ε_i) is given in eq 4

$$\varepsilon_i = \left\{ \left[\frac{\lambda^3(1-f)+\lambda^2 f}{1-f+\lambda^2 f} \right]^{1/3} - 1 \right\} \frac{100}{\lambda - 1} \qquad (4)$$

where λ is the extension ratio imposed and f is the fractional stress remaining after time t_s, obtained from stress−relaxation curves such as those shown in Figure 16 for determining τ_3.

Permanent Set in High Strain Regime. Permanent set in high strain regime was determined by measuring the dimensions of the sample after 30 min of removal of the sample from the constraint. The permanent set was calculated based on eq 5:

$$\varepsilon_p = \frac{l_s - l_u}{l_x - l_u} \qquad (5)$$

where ε_p is the permanent set, l_s the set length, l_u the unstretched length, and l_x the stretched length. The instantaneous set and the permanent set are plotted against the increase in λ^c as shown in Figure 18. As λ^c increases, the permanent set decreases significantly, indicating that the double network elastomers exhibit low permanent set, as compared to the sample cured at $\lambda^c = 1$, even in the high strain regime. This is also due to the fact that both the relaxation behavior is dominated by physical relaxation and the retracting force of first network increases as it moves further away from its equilibrium state with increase in λ^c. Hence, these competitive network elastomers show a lower permanent set in both low and high strain regime.

The individual contribution of the three different relaxation processes and their relationship to network structure, especially the relaxation process corresponding to τ_2, has to be studied in much more detail and will be discussed in future publications.

Mechanical Hysteresis in Double Network Elastomers. From the cyclic tests shown in Figure 18, it is evident that the cured samples behavior similar to the "Mullins effect" observed for filled rubbers. However, there is a significant difference in the second and subsequent cycle hysteresis. The hysteresis of the second cycle in the single network system ($\lambda^c = 1$) is still rather substantial. In the case of competitive network elastomer, the hysteresis of the second cycle is greatly reduced and decreases with increase in λ^c. This decrease in dissipation may be attributed to the heat exchange within the system between the two networks, rather than with the surroundings, although further studies are necessary to confirm this result. Nonetheless, it should be noted that there is a consistent measured decrease that continues with increase in λ^c, even having higher extent of cross-linking as shown in Figure 19. This result is consistent with the hypothesis that the decrease is due to a reduction of heat exchange with the surroundings. In addition, the strain recovery behavior of these

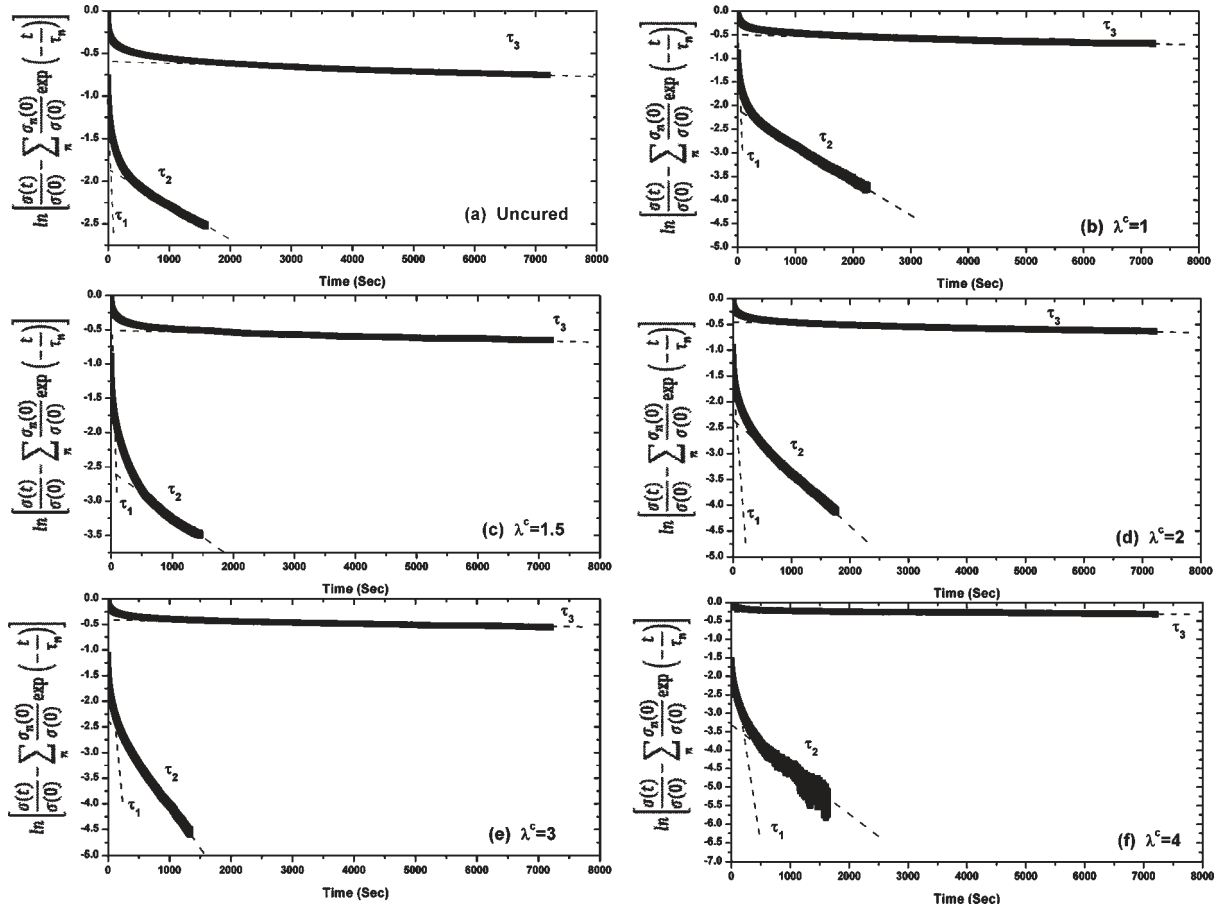

Figure 16. Separation of stress relaxation of double and single network elastomers using procedure X in high strain regime.

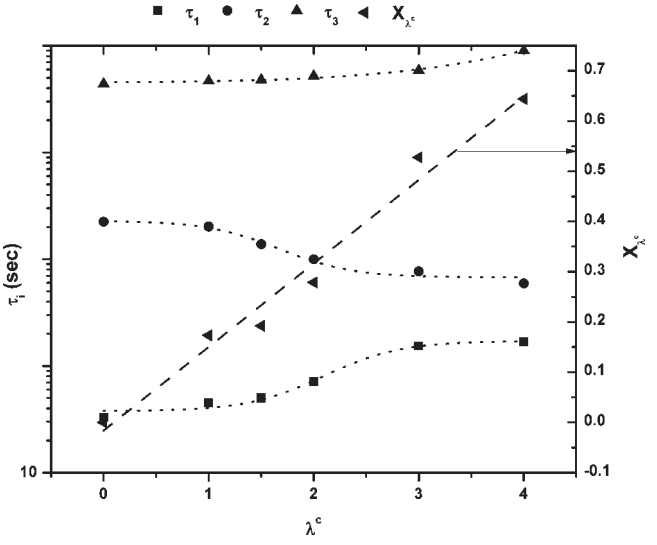

Figure 17. Time constants τ_1, τ_2, and τ_3 as a function of λ^c and their relationship with extent of cure during stretch (X_λ^c) in high strain regime.

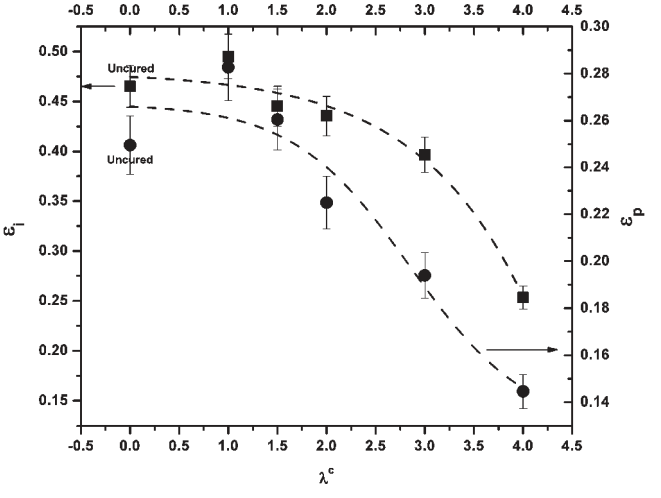

Figure 18. Change in instantaneous set (ε_i) and permanent set (ε_p) in the sample with change in λ^c in the high strain regime.

double network elastomers supports the decrease in hysteresis. This decrease in hysteresis may also increase the fatigue life of the competitive network elastomer even with higher cross-link density, as earlier reported by Roland et al.[22]

Thermomechanical Analysis. The dimensional change measured at constant load as a function of temperature is shown in Figure 21. The coefficient of linear thermal expansion (α) was calculated using eq 6

$$\alpha = \frac{\Delta L K}{\Delta T L} \qquad (6)$$

where α is the coefficient of expansion (μm/mm°C), L is the sample length (mm), ΔL is the change in sample length (μm), ΔT is the change in temperature (°C), and K is the cell constant

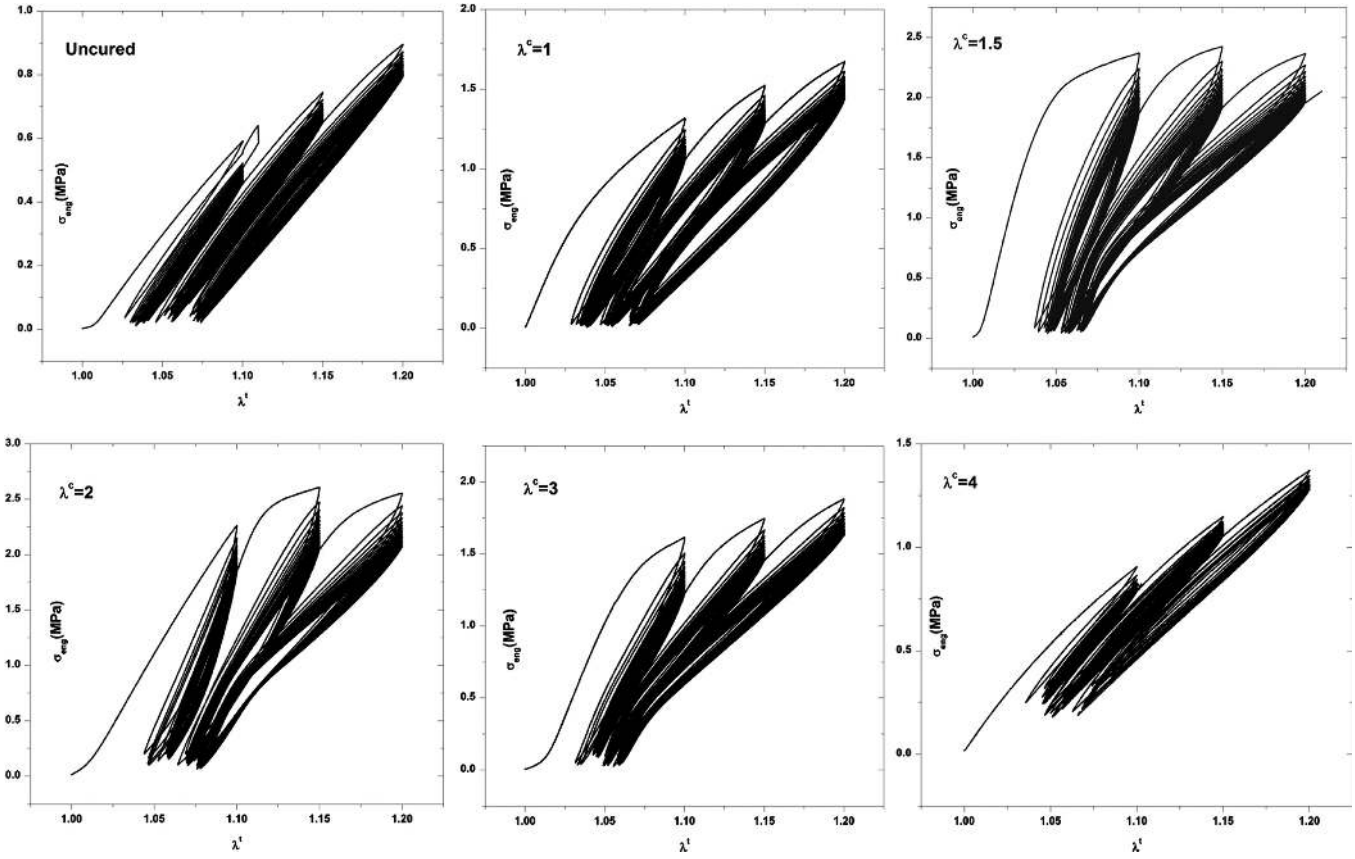

Figure 19. Cyclic tests of competitive double network elastomers.

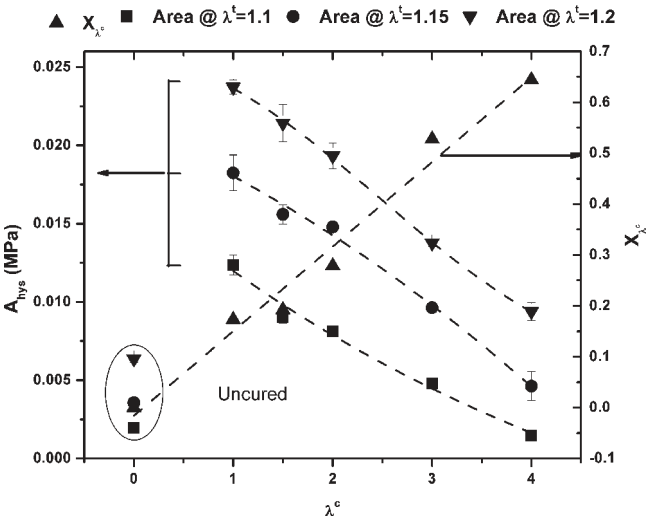

Figure 20. Relationship of hysteresis area under the curve (A_{hys}) with λ^c and extent of cure during stretch ($X_\lambda{}^c$) at various λ^t.

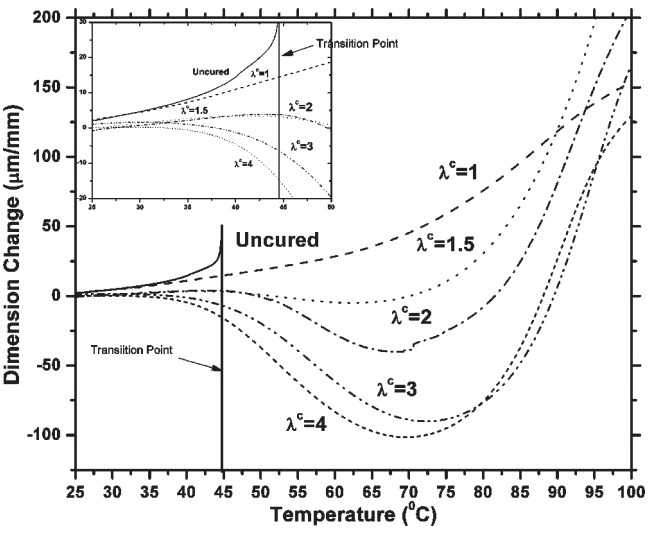

Figure 21. TMA results of double network samples cured at different λ^c at constant load of 0.05 N and temperature ramp rate of 3 °C/min.

of the instrument. It is evident that the curing at $\lambda^c = 1$ leads to a decrease in α of SBS and an improved thermal stability under load as compared to the uncured sample. Hence, it may be suitable for high-temperature applications.

It is also evident that the samples cured at various λ^c show interesting behavior along with increase in temperature. All the samples with $\lambda^c = 1-4$ show a transition at ~45−50 °C, at which only the physically cross-linked uncured samples failed.

It is evident from Figure 22 that the α values before the transition point are positive for the sample cured at $\lambda^c = 1$. The samples cured at higher λ^c show a decrease in α, and in the case of $\lambda^c = 4$, it almost reaches zero. They show a transition at ~45−50 °C, beyond which a negative α is obtained. This can be attributed to that fact that below the transition point the second network is leading to increase in anisotropy of first network in the direction of stretch due to an increase in residual strain. However, beyond the transition point,

dx.doi.org/10.1021/ma1028054 |*Macromolecules* 2011, 44, 1480–1490

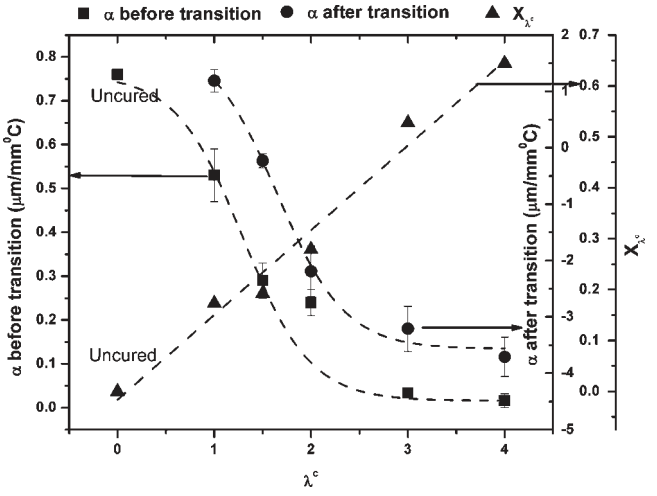

Figure 22. α of SBS competitive double network elastomers before and after the transition point with increase in extent of cure (X_λ^c) at various λ^c.

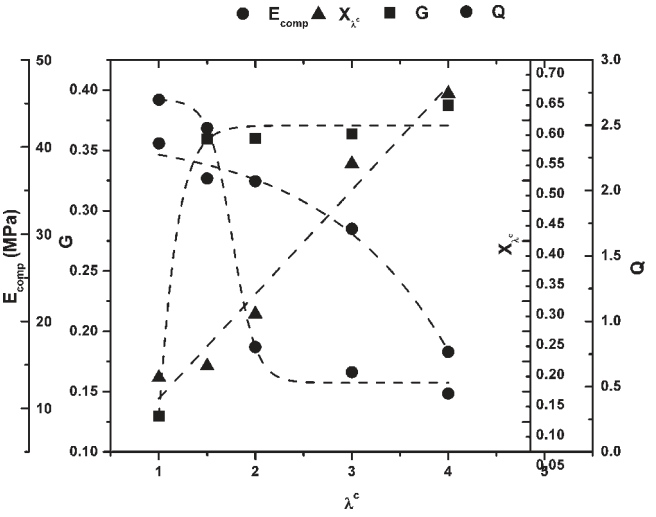

Figure 23. Change in gel fraction (G) and swelling ratio (Q) with increase in λ^c of SBS based competitive double network elastomers and their relationship to extent of cure during stretch (X_λ^c) and the initial modulus (E_{comp}).

where first network fails, the second network tries to attain equilibrium and, following entropic behavior, contracts, which is seen as a negative α value. The negative α values also increase with increasing λ^c due to increase in residual strains. Beyond ~70 °C there is an expansion observed, which might be due to the overall expansion of both the networks together.

The explanation of this kind of behavior of elastomers has been observed by Joule,[60] where elastomers show a contraction when they are under strain. The double network elastomers are inherently under strain, and the decrease in coefficient of thermal expansion can be explained by the *thermoelastic inversion*.[1] Joule calculated the change in temperature using the variant of eq 7.

$$\Delta T_{ad} = -\left(\frac{T}{jc_p w}\right)\left[\frac{1}{L}\left(\frac{\partial L}{\partial T}\right)_{P,f}\right]\Delta f \qquad (7)$$

There was a sign reversal of $(\delta L/\delta T)_{P,f}$ occurring at low elongation, resulting in inversion of ΔT. This inversion in the sign of ΔT may be regarded as a essential outcome of the fact that the linear coefficient of expansion of strained rubber is negative, while that of unstrained rubber is positive. Similar behavior is also explained earlier by Meyer et al.[61] and Elliott et al.[62] Hence, the double networks having stretched chains, frozen in the system, by introducing the second network in stretched state, lead to contraction upon heating, which increases with increase in cross-linking densities with λ^c as shown in Figure 22. This leads to overall decrease in linear coefficient of thermal expansion.

Swelling. The gel fraction and swelling ratio were calculated from the measured weights before, during, and after swelling using eq 8 and 9 respectively.

$$G = \frac{W_D}{W_I} \qquad (8)$$

$$Q = \frac{W_S}{W_D} \qquad (9)$$

where G is the gel fraction, Q the swelling ratio, W_D the weight after drying, W_I the initial weight, and W_S the weight after swelling. The change in gel fraction and swelling ratios with respect to λ^c is shown in Figure 23. As λ^c increases, there is an increase in the gel fraction and decrease in the swelling ratio. This indicates that the double network elastomers follow the extent of cross-linking, and hence with increase in degree of cross-linking there is an increase in gel fraction and decrease in swelling ratio. The sample cured at $\lambda^c = 4$ even shows shrinkage, which is an interesting result and needs further experiments to elucidate the mechanism, which is out of scope of current paper and will be discussed in future publications.

Hence, it is evident that the competitive double network elastomers results in materials with higher cross-link density with improved swelling properties but still resulting in lower initial modulus as shown in Figure 23.

CONCLUSION

SBS-based double networks have been synthesized and investigated. In these systems, a competitive regime and a collaborative regime have been identified, and the transition point is related to the elongation of the sample during the formation of the second network. It is observed that with an increase in λ^c there is an increase in degree of cross-linking, but the initial modulus does not follow the extent of cross-linking and decreases with increase in λ^c. This can be attributed to the competitive nature of the networks. Beyond a transition point there is an increase in the modulus with increase in λ^c that can be attributed to the collaborative nature of these networks and satisfies the independent network hypothesis. These results confirm earlier studies where similar behavior was observed by tensile and DMA testing of SEBS and EPDM systems.[8]

From the stress relaxation experiments, it is observed that these competitive networks result in low permanent set in low as well as high strain regime due to physical relaxation processes of both the rubbery and glassy phases and the difference between the two strain regimes lie in the relaxation of trapped confinements and are also related to morphological structure of double network elastomer. This relationship is being probed in detail currently. Coincidently, these competitive network elastomers also show lower extent of mechanical hysteresis, which is also related to lower permanent set, which is attributed to heat

transfer within the system between two networks, rather than with the surroundings, leading to low dissipation. Moreover, these networks show lower degree of swelling, with increase in λ^c, following overall degree of cross-linking. These double network elastomers also show low coefficient of thermal expansion due to competitive nature of the two networks. Hence, from this work it is evident that a simple process modification of SBS triblock copolymer during cross-linking can result in a material, with unique set of properties, with high cross-linking density, lower swelling but still having lower modulus, lower hysteresis similar uncured triblock copolymer, lower permanent set, and low CTE similar to cured elastomer, which is very difficult to achieve in a single material. This can be utilized in applications where temperature stability and lower swelling are required by a soft elastomer.

AUTHOR INFORMATION

Corresponding Author

*E-mail: ajl@polysci.umass.edu.

ACKNOWLEDGMENT

We thank Kathryn Wright, KRATON Polymers LLC, for providing the materials used in this study and kind discussions on the results.

REFERENCES

(1) Flory, P. J. *Principles of Polymer Chemistry*; Cornell University Press: Ithaca, NY, 1953.
(2) Roland, C. M.; Warzel, M. L. *Rubber Chem. Technol.* **1990**, *63*, 285.
(3) Santangelo, P. G.; Roland, C. M. *Rubber Chem. Technol.* **1994**, *67*, 359.
(4) Andrews, R. D.; Tobolsky, A. V.; Hanson, E. E. *J. Appl. Phys.* **1946**, *17*, 352.
(5) Baldwin, F. P.; W., N. J. US Patent 2488112, 1945.
(6) Erman, B. *Biol. Synth. Polym. Networks* **1988**, *497*, 497.
(7) Singh, N. K.; Lesser, A. J. In *Annual Technical Conference - Society of Plastic Engineers*, Chicago, 2009; Vol. 67, p 868.
(8) Singh, N. K.; Lesser, A. J. *J. Polym. Sci., Part B: Polym. Phys.* **2010**, *48*, 778.
(9) Singh, N. K.; Lesser, A. J. In *Annual Technical Conference - Society of Plastic Engineers*, Orlando, 2010; Vol. 68.
(10) Lesser, A. J.; Singh, N. K.; Mamodia, M. US Patent Application Number US20100286304, 2010; 38 pp.
(11) Aprem, A. S.; Joseph, K.; Thomas, S. *J. Appl. Polym. Sci.* **2004**, *91*, 1068.
(12) Gillen, K. T. *Macromolecules* **1988**, *21*, 442.
(13) Kaang, S.; Gong, D.; Nah, C. *J. Appl. Polym. Sci.* **1997**, *65*, 917.
(14) Kaang, S.; Gong, D.; Nah, C.; Kim, S.; Kim, J. M. *Polymer (Korea)* **1997**, *21*, 282.
(15) Kaang, S.; Nah, C. *Polymer* **1998**, *39*, 2209.
(16) Marykut-Ry, C. V.; Mathew, G.; Thomas, S. *Rubber Chem. Technol.* **2007**, *80*, 809.
(17) Mott, P. H.; Roland, C. M. *Macromolecules* **2000**, *33*, 4132.
(18) Roland, C. M.; Santangelo, P. G. World Patent 95/26367, 1995.
(19) Roland, C. M.; Peng, K. L. *Rubber Chem. Technol.* **1991**, *64*, 790.
(20) Santangelo, P. G.; Roland, C. M. *Rubber Chem. Technol.* **1995**, *68*, 124.
(21) Santangelo, P. G.; Roland, C. M. *Rubber Chem. Technol.* **2003**, *76*, 892.
(22) Wang, J.; Hamed, G. R.; Umetsu, K.; Roland, C. M. *Rubber Chem. Technol.* **2005**, *78*, 76.
(23) Twardowski, T.; Kramer, O. *Macromolecules* **1991**, *24*, 5769.
(24) Carpenter, R. L.; Kramer, O.; Ferry, J. D. *Macromolecules* **1977**, *10*, 117.
(25) Kramer, O.; Ferry, J. D. *J. Polym. Sci., Part B: Polym. Phys.* **1977**, *15*, 761.
(26) Hvidt, S.; Kramer, O.; Batsberg, W.; Ferry, J. D. *Macromolecules* **1980**, *13*, 933.
(27) Flory, P. J. *Trans. Faraday Soc.* **1960**, *56*, 722.
(28) Kramer, O.; Ty, V.; Carpente, Rl; Ferry, J. D. *Bull. Am. Phys. Soc.* **1973**, *18*, 318.
(29) Kramer, O.; Carpenter, R. L.; Ty, V.; Ferry, J. D. *Macromolecules* **1974**, *7*, 79.
(30) Carpenter, R. L.; Kramer, O.; Ferry, J. D. *Bull. Am. Phys. Soc.* **1977**, *22*, 429.
(31) Carpenter, R. L.; Kramer, O.; Ferry, J. D. *J. Appl. Polym. Sci.* **1978**, *22*, 335.
(32) Berry, J. P.; Scanlan, J.; Watson, W. F. *Trans. Faraday Soc.* **1956**, *52*, 1137.
(33) Hamed, G. N.; Huang, M. Y. *Rubber Chem. Technol.* **1998**, *71*, 846.
(34) Hamed, G. R.; Huang, M. Y. *Rubber Chem. Technol.* **1998**, *71*, 846.
(35) Hamed, G. R.; Umetsu, K. *Rubber Chem. Technol.* **2005**, *78*, 130.
(36) Ohlemacher, C. J.; Hamed, G. R. *Rubber Chem. Technol.* **2008**, *81*, 650.
(37) Flory, P. J. *Chem. Rev.* **1944**, *35*, 51.
(38) James, H. M.; Guth, E. *J. Chem. Phys.* **1947**, *15*, 669.
(39) Baxandall, L. G.; Edwards, S. F. *Macromolecules* **1988**, *21*, 1763.
(40) Budzien, J.; Rottach, D. R.; Curro, J. G.; Lo, C. S.; Thompson, A. P. *Macromolecules* **2008**, *41*, 9896.
(41) Flory, P. J. *J. Am. Chem. Soc.* **1956**, *78*, 5222.
(42) Meissner, B.; Matjka, L. *Polymer* **2003**, *44*, 4611.
(43) Okumura, K. *Europhys. Lett.* **2004**, *67*, 470.
(44) Rottach, D. R.; Curro, J. G.; Budzien, J.; Grest, G. S.; Svaneborg, C.; Everaers, R. *Macromolecules* **2006**, *39*, 5521.
(45) Rottach, D. R.; Curro, J. G.; Budzien, J.; Grest, G. S.; Svaneborg, C.; Everaers, R. *Macromolecules* **2007**, *40*, 131.
(46) Rottach, D. R.; Curro, J. G.; Grest, G. S.; Thompson, A. P. *Macromolecules* **2004**, *37*, 5468.
(47) Svaneborg, C.; Everaers, R.; Grest, G. S.; Curro, J. G. *Macromolecules* **2008**, *41*, 4920.
(48) Gong, J. P. *Soft Matter* **2010**, *6*, 2583.
(49) Gong, J. P.; Katsuyama, Y.; Kurokawa, T.; Osada, Y. *Adv. Mater. (Weinheim, Ger.)* **2003**, *15*, 1155.
(50) Bosch, P.; Mateo, J. L.; Serrano, J. *J. Photochem. Photobiol., A* **1997**, *103*, 177.
(51) Decker, C.; Trieu, N. T. V. *Macromol. Chem. Phys.* **1999**, *200*, 358.
(52) Mamodia, M.; Indukuri, K.; Atkins, E. T.; De, J. W. H.; Lesser, A. J. *J. Mater. Sci.* **2008**, *43*, 7035.
(53) Hsiue, G. H.; Chen, D. J.; Liew, Y. K. *J. Appl. Polym. Sci.* **1988**, *35*, 995.
(54) Wu, G. W.; Hsiue, G. H.; Yang, J. S. *Mater. Chem. Phys.* **1994**, *37*, 191.
(55) Wu, G.-W.; Hsiue, G.-H.; Yang, J.-S. *Mater. Chem. Phys.* **1994**, *39*, 29.
(56) Indukuri, K. K.; Lesser, A. J. *Polymer* **2005**, *46*, 7218.
(57) Tobolsky, A. V.; Murakami, K. *J. Polym. Sci.* **1959**, *40*, 443.
(58) Mandare, P.; Horst, R.; Winter, H. H. *Rheol. Acta* **2005**, *45*, 33.
(59) Shimizu, K.; Saito, H. *Polym. J. (Tokyo, Jpn.)* **2009**, *41*, 562.
(60) Joule, J. P. *Philos. Trans. R. Soc. London* **1859**, *A149*, 91.
(61) Meyer, K. H.; Ferri, C. *Helv. Chim. Acta* **1935**, *18*, 570.
(62) Elliott, D. R.; Lippmann, S. A. *J. Appl. Phys.* **1945**, *16*, 50.